A comparison of the MR-TSOM and DBIM in reconstructing 2D model of human breast

Xiuzhu YE
Department of Electronics and Information Engineering
Beihang University
Beijing, China
yexiuzhu@buaa.edu.cn

Kuiwen Xu
Department of Electronics and Information Engineering
Hangdian University
Beijing, China
kuiwenxu@hdu.edu.cn

***Abstract*—This article reconstructs the two-dimensional simplified breast cancer phantom by using two different inversion methods: the distorted-Born iterative method (DBIM) and the multiplicative-regularization two-folded subspace-based optimization method (MR-TSOM). The frequency selected is 300MHz, and the dielectric parameters are modeled according to the real data. Liquid matching layer is also modeled with real dielectric parameter, to make sure that the microwave is guided into the breast. It is shown that the two methods are both able to locate and distinguish the malignant cells from the benign ones through the contrast of dielectric permittivity. The convergence rate and the reconstruction errors of the two methods are compared at last.**

Keywords—breast cancer;microwave imaging

INTRODUCTION

Breast cancer is the killer of hundreds of thousands women annually in the world. The early stage detection of the malignant cells is of key importance in curing the cancer and ensuring the survival of the patients [1]. There are several existing methods such as X-ray mammography, magnetic resonance imaging (MRI), and ultrasound imaging commonly used for diagnosing the breast cancer. However, the X-ray mammography is highly ionizing radiative and the patients' breasts are usually compressed by the two plates during the imaging process, which usually produces uncomfortable pain. Besides, even though the imaging resolution is high for X-ray, the contrast between the malignant and benign cell is quite low which results in high false diagnose rate [2]. The ultrasound imaging is safe and painless. However, the image usually contains many artifacts and ambiguities and requires high-skilled and experienced operators to read the image. The MRI is good in image quality, however is quite expensive for patients in developing countries to take regular exams [3].

Microwave tomography imaging is a suitable candidate for breast cancer imaging due to its non-ionizing radiation and high dielectric contrast between the benign and malignant cells in the microwave frequency range [4, 5]. This article is devoted to testing the effectiveness of two inverse scattering algorithms in reconstructing a 2-D simplified phantom of breast cancer. One is the multiplicative-regularization two-folded subspace-based optimization method (MR-TSOM) and the other is the distorted-Born iterative method (DBIM). The MR-TSOM is a typical source-type inversion algorithm and the DBIM is a typical field-type inversion algorithm. The DBIM is already proven to be effective in the medical imaging for breast cancer [6]. While the SOM related algorithms have never been used in the biomedical imaging yet. Therefore, the focus of this article is on testing the effectiveness of MR-TSOM and making a comparison with DBIM on the convergence and reconstructing accuracy.

FORWARD MODEL

A. Simplified two-dimensional breast phantom

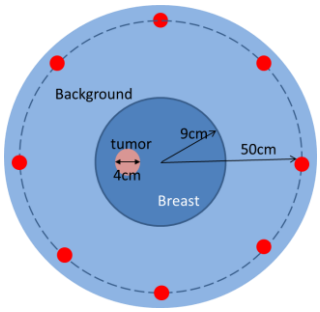

Figure 1. Simplified 2D breast phantom

As depicted in Figure 1. The 2-D simplified breast phantom has a layer of unified fat tissue. It is assumed that there is a tumor embedded inside the breast. The frequency we choose is 300MHz. The background medium is composed by the matching liquid which guides the microwave inside the breast. The real part and imaginary part of the dielectric relative permittivity is given in Table 1, which is calculated according to the real breast data [3, 7, 8]. The skin layer is neglected here.

TABLE I.
THE DIELECTRIC PROPERTY OF THE BREAST PHANTOM

Tissue	ε'	ε''
Background	34	0
Breast	39	4.35
Tumor	60	5

B. Forward model

Here, a 2-D inverse scattering problem with the transverse magnetic (TM) incidence is considered. All the electric fields and currents are in the longitudinal direction z only. The model consists of a bounded domain D , where the unknown scatterers are of permittivity $\varepsilon(\mathbf{r})$, $\mathbf{r} \in D$, and the background

homogeneous medium with permittivity ε_b, permeability μ_b and wavenumber $k_b = \omega(\varepsilon_b\mu_b)^{1/2}$. The contrast function of the unknown scatterers can be defined as, $\chi = (\varepsilon(\mathbf{r}) - \varepsilon_b)/\varepsilon_b$. The domain D is illuminated by N_i monochromatic plane waves $E_l^{inc}(\mathbf{r})$, l = 1, 2, …, N_i. For each incidence, scattered electric fields $E_l^{sca}(\mathbf{r})$ are collected by N_r receivers uniformly distributed on the observation domain S, with the position $\mathbf{r}^s_q$, q = 1, 2, …, N_r. Thus, there are totally N_iN_r data points of measurement recorded in the scattered field matrix. The test domain D in the *x-y* plane is discretized into rectangular subunits centered at $\mathbf{r}_m$. The total number of subunits is M.

INVERSION ALGORITHMS

The purpose of the inversion algorithm is to reconstruct the electromagnetic properties of the object under detection using the measured scattered field data. In this scenario, the object to be reconstructed is the breast phantom.

A. Distorted Born Iterative Method

In the updating process of DBIM, the difference of contrast compared to the profile reconstructed in the last step is the unknown to be reconstructed. The reconstructed profile of the last step is considered as the inhomogeneous background medium and the Green's function for this inhomogeneous background is also updated accordingly. The total electric field inside the domain of interest is approximated by the scattered field produced by the inhomogeneous background. The iterative process is omitted here and the reads can refer to [9] for details.

B. Multiplicative-Regularization Two-Folded Subspace-Based Optimization Method

In the following, a quick review of the TSOM would be introduced, and more details can be found in [11]. The induced contrast sources in SOM can be decomposed into deterministic part of the induced current (DPIC) $\bar{I}^{\mathrm{d}}$ and ambiguous part of the induced current (APIC) $\bar{I}^{\mathrm{a}}$.

By discretizing Lippmann–Schwinger equation, the contrast sources can be expressed as

$$\bar{I}_l^{\mathrm{d}} + \bar{I}_l^{\mathrm{a}} = -i\omega\varepsilon_b\bar{\bar{\chi}}\cdot(\bar{E}_l^{inc} + \bar{\bar{G}}_D\cdot\bar{I}^{\mathrm{d}} + \bar{\bar{G}}_D\cdot\bar{I}^{a}) \tag{1}$$

where $\bar{\bar{G}}_D$ is the internal radiation operator mapping the induced current sources within D to scattered fields within D. And the scattered fields in the observation domain S can be written as:

$$\bar{E}_l^{sca} = \bar{\bar{G}}_s\cdot\left(\bar{I}_l^{\mathrm{d}} + \bar{I}_l^{\mathrm{a}}\right) \tag{2}$$

Where $\bar{\bar{G}}_s$ is the operator mapping the induced current sources within D to scattered fields on the observation domain S, Equations (1) and (2) are usually referred to as state equation and data equation, respectively.

With the spectral information from the SVD of $\bar{\bar{G}}_s$, the DPIC can be obtained as,

$$\bar{I}_l^{\mathrm{d}} = \sum_{j=1}^{L}\frac{\bar{u}_j^{S*}\cdot\bar{E}_l^{sca}}{\sigma_j^S}\bar{v}_j^s = \bar{\bar{V}}_S^{+}\cdot\bar{\alpha}_l^{+} \tag{3}$$

Where $\bar{\bar{V}}_S^{+} = [\bar{v}_1^s, \bar{v}_2^s, ..., \bar{v}_L^s]$, and $\bar{\alpha}_l^{+} = [\bar{\alpha}_{l;1}^{+}, \bar{\alpha}_{l;2}^{+}, ..., \bar{\alpha}_{l;L}^{+}]$, $\bar{\alpha}_{l;j}^{+} = (\bar{u}_j^{S*}\cdot\bar{E}_l^{sca})/\sigma_j^s$, j = *1, 2, ..., L*, superscript * denotes the Hermitian operation, whereas superscript + refers to the dominant current space, the subspace corresponding to the dominant singular values. The value of L is chosen according to the singular values of $\bar{\bar{G}}_s$ and the level of the noise. We can express the APIC as

$$\bar{I}_l^{\mathrm{a}}(\bar{\beta}_l) = \bar{\bar{\mathrm{V}}}_D^{+'}\cdot\bar{\beta}_l \tag{4}$$

where $\bar{\beta}_l$ is an M_0-dementional vector, and the current subspace $\bar{\bar{\mathrm{V}}}_D^{+'} = [\bar{\bar{I}}_M - \bar{\bar{V}}_S^{+}\cdot\bar{\bar{V}}_S^{+*}]\cdot\bar{\bar{V}}_D^{+}$, $\bar{\bar{\mathrm{V}}}_D^{+} = [\bar{v}_1^D, \bar{v}_2^D, ..., \bar{v}_{M_0}^D]$ is the current subspace spanned by the singular vectors to the largest M_0 singular values of the operator $\bar{\bar{G}}_D$.

After constructing the induced current sources, the cost function of the TSOM can be defined as follows,

$$f_T(\bar{\beta}_l, \bar{\bar{\chi}}) = \sum_{l=1}^{N_i}\left(\frac{\Delta_l^{fie}(\bar{\beta}_l)}{\left\|\bar{E}_l^{sca}\right\|^2} + \frac{\Delta_l^{cur}(\bar{\beta}_l, \bar{\bar{\chi}})}{\left\|\bar{E}_l^{inc}\right\|^2}\right) \tag{5}$$

where $\|\cdot\|$ is the Euclidean length of a vector. The residue in the state equation (1) and the data equation (2) can be expressed as, $\Delta_l^{fie}(\bar{\beta}_l) = \left\|\bar{E}_l^{sca} - \bar{\bar{G}}_s\cdot\left(\bar{I}_l^{\mathrm{d}} + \bar{I}_l^{\mathrm{a}}\right)\right\|^2$ and $\Delta_l^{cur}(\bar{\beta}_l, \bar{\bar{\chi}}) = \left\|\bar{L}(\bar{\beta}_l) - \bar{\Gamma}_l\right\|^2$, where $\bar{L}(\bar{\beta}_l) = \bar{I}_l^{\mathrm{a}}/(-i\omega\varepsilon_b) - \bar{\bar{\chi}}\cdot(\bar{\bar{G}}_D\cdot\bar{I}_l^{\mathrm{a}})$ and $\bar{\Gamma}_l = \bar{\bar{\chi}}\cdot(\bar{E}_l^{inc} + \bar{\bar{G}}_D\cdot\bar{I}_l^{\mathrm{d}}) + \bar{I}_l^{\mathrm{d}}/(i\omega\varepsilon_b)$.

To further stabilize the solution of the ISP, the multiplicative regularization (MR) technique is introduced in the TSOM, denoted as MR-TSOM. Herein, the multiplicative regularizer with a weighted L_2-norm total variation (TV) is used. In the MR-TSOM method, the objective function is composed of the original cost function (5), and a new term, multiplicative regularizer. With the inclusion of the multiplicative regularizer, the objective function, can be defined as

$$\mathrm{H}_n(\bar{\beta}_l, \bar{\bar{\chi}}) = f_T(\bar{\beta}_l, \bar{\bar{\chi}})\cdot\mathbb{F}_n^{TV}\left(\bar{\bar{\chi}}\right) \tag{6}$$

where $\bar{\beta}_l$, $\bar{\bar{\chi}}$ are the unknowns and the multiplicative regularizer is given as

$$\mathbb{F}_n^{TV}\left(\bar{\bar{\chi}}\right) = \frac{1}{A}\int_D\frac{\left|\nabla\chi_n\right|^2 + \delta_n^2}{\left|\nabla\chi_{n-1}\right|^2 + \delta_n^2}dv \tag{7}$$

where A is the area of the test domain D, and ∇ denotes the spatial differentiation with respect to **r**. The constant regularization parameter δ^2_n is introduced for restoring differentiability of the TV regularization. From [10], the effect of the regularization should be increased as a function of the number of the iterations by decreasing the regularization parameter, the regularization parameter is chosen as follows:

$$\delta_n^2 = \frac{F_s(\bar{\beta}_l, \bar{\bar{\chi}})}{\Delta^2} \times \Lambda(n) \tag{8}$$

where $F_s(\bar{\beta}_l, \bar{\bar{\chi}}) = \Delta_l^{cur}(\bar{\beta}_l, \bar{\bar{\chi}}) \Big/ \left\| \bar{\bar{E}}_l^{inc} \right\|^2$ and Δ is the mesh size of the discretized D. The auxiliary function $\Lambda(n)$ should be well designed to guarantee that δ^2_n is gradually reduced to a threshold, which can make sure that the inverse scattering problem remains convex.

NUMERICAL RESULTS

The number of illuminating antennas used is 10 and number of receiving antennas is 30, both of which are supposed to work inside the background liquid evenly distributed around a circle with radius 0.5m. As shown in Figure 2 and 3, both DBIM and MR-TSOM are able to reconstruct the tumor inside breast. The reconstruction error for relative permittivity is as defined in Eq. (9). The convergent curves for both DBIM and MR-TSOM are as shown in Figure 4.

$$\frac{\sum_{i=1}^{M} \mathrm{abs}\left(\left| (\varepsilon' + \mathrm{i}\,\varepsilon'')_{i,\,\mathrm{reconstructed}} \right| - \left| (\varepsilon' + \mathrm{i}\,\varepsilon'')_{i,\,\mathrm{original}} \right| / \left| (\varepsilon' + \mathrm{i}\,\varepsilon'')_{i,\,\mathrm{original}} \right| \right)}{M} \tag{9}$$

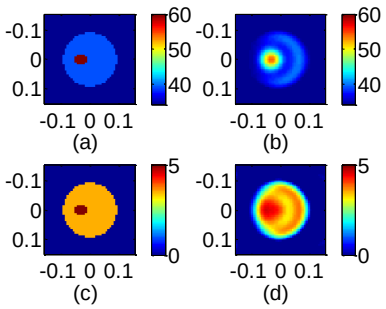

Figure 2. Numerical result got by DBIM: (a) the original pattern of real part (b) the reconstructed pattern of real part (c) the original pattern of imaginary part (d) the reconstructed pattern of imaginary part, of the relative permittivity

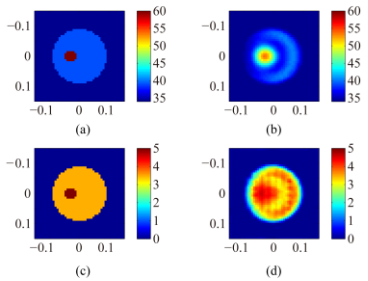

Figure 3. Numerical result got by MR-TSOM: (a) the original pattern of real part (b) the reconstructed pattern of real part (c) the original pattern of imaginary part (d) the reconstructed pattern of imaginary part, of the relative permittivity

TABLE II.
THE RECONSTRUCTION ERRORS

	Relative error
DBIM	0.0164
MR-TSOM	0.0170

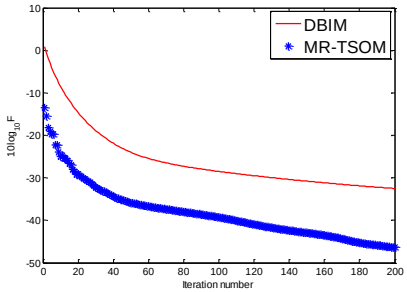

Figure 4. convergence of the two methods

ACKNOWLEDGMENT

This work was supported by the National Natural Science Fund of China under Grant No. 61401009 and No. 61601161.

III. REFERENCES

[1] Wikipedia, *Breast cancer*, https://en.wikipedia.org/wiki/Breast_cancer

[2] A. Berrington de González and S. Darby, "Risk of cancer from diagnostic x-rays: estimates for the UK and 14 other countries," *Lancet*, vol. 363, no. 9406, pp. 345–351, 2004.

[3] M. G. Garcia "Multi-Antenna Multi-Frequency Microwave Imaging Systems for Biomedical Applications", *doctoral thesis*, 2013.

[4] L. Jofre, M. Hawley, A. Broquetas, E. de los Reyes, M. Ferrando, and A. Elias-Fuste, "Medical imaging with a microwave tomographic scanner," *IEEE Transactions on Biomedical Engineering*, vol. 37, no. 3, pp. 303 – 312, march 1990

[5] C. Gilmore, P. Mojabi, A. Zakaria, S. Pistorius, and J. LoVetri, "On super-resolution with an experimental microwave tomography system," *IEEE Antennas and Wireless Propagation Letters*, vol. 9, pp. 393–396, 2010.

[6] Fuqiang Gao, Barry D. Van Veen, and Susan C. Hagness, "Sensitivity of the Distorted Born Iterative Method to the Initial Guess in Microwave Breast Imaging," *IEEE Transactions on Antennas and Propagation*, Vol. 63, no. 8, pp. 3540-3547, 2015.

[7] S. Gabriel, R. W. Lau, and C. Gabriel, "The dielectric properties of biological tissues Ii: .measurements in the frequency range 10Hz to 20GHz," *Phys. Med. Biol*., vol. 41, no. 11, pp. 2251, 1996.

[8] D. Andreuccetti, R. Fossi, and C. Petrucci. (1997-2012) Calculation of the dielectric properties of body tissues in the frequency range 10Hz - 100 GHz. IFAC-CNR. Florence (Italy).

[9] W. C. Chew and Y. M. Wang, "Reconstruction of two-dimensional permittivity distribution using the distorted-Born iterative method," *IEEE Transactions on Medical Imaging*, vol. 9, pp. 218-225, 1990.

[10] K. Xu, Y. Zhong, R. Song, X. Chen, and L. Ran, "Multiplicative-regularized FFT twofold subspace-based optimization method for inverse scattering problems," *IEEE Transactions on Antennas and Propagation*, Vol. 53, no. 2, pp. 841-850, 2015.

[11] Y. Zhong and X. Chen, "An FFT twofold subspace-based optimization method for solving electromagnetic inverse scattering problems," IEEE Transactions on Antennas and Propagation, vol. 59, no. 3, pp. 914–927, 2011